NEAR-SURFACE HEATING ON ENCELADUS AND THE SOUTH POLAR THERMAL ANOMALY. J. H. Roberts[1], F. Nimmo[1], [1]Department of Earth and Planetary Science, UC Santa Cruz, 1156 High Street, Santa Cruz, CA 95064-1077. Corresponding Author's Email: jhr@ucsc.edu

Introduction: The south polar terrain on Enceladus is a region of depressed topography [1], a heat flow anomaly [2], and tectonic and plume activity [3]. Tidal dissipation in the ice shell is a leading candidate for the source of the 4-7 GW of heat observed in this region [2]. Tidal heating is efficient if the ice shell is mechanically decoupled from the silicate core, but cannot explain the localized observed heat flow [4]. Strike-slip motion due to diurnal tidal stresses [5] may lead to localized near-surface shear heating along fractures (e.g. the Tiger-stripes) through viscous dissipation or friction [6], and may account for the observed heat flow [7].

Here, we investigate the effect of near-surface heating on the underlying convection [8], dynamic topography, melt production and subsidence. We also seek to explain the polar location of the thermal anomaly, and examine the degree to which the convective pattern and topography could have promoted true polar wander (TPW) [9].

Modeling: We considered an Enceladus model with three material layers: a 160-km silicate core, and a liquid water ocean and ice shell with combined thickness of 90 km. We computed the background tidal heating in the ice shell [4,10,11].

We modeled convection in the ice shell in a axisymmetric spherical geometry using the finite-element code Citcom [12]. We used the Boussinesq approximation, and applied free-slip boundary conditions at the top and bottom. The bottom boundary is isothermal at 273 K. The surface temperature varies with latitude [13] from 75 K at the equator to 57 K at the poles. The ice shell is heated internally by the tidal heat distribution calculated above. The tidal heat at each point is perturbed at every timestep based on the local viscosity, η [13,14], which is a function of temperature, T:

$$\eta = \eta_0 \exp (E/RT) \qquad (1)$$

where η_0 is the viscosity at the bottom, E is the activation energy, and R is the gas constant.

To examine the effect of near-surface heating, we imposed an additional 7 GW of heat in the top 5 km of the ice shell, distributed in a $\sin^2\theta$ pattern, poleward of 55º S, where θ is the co-latitude. The pole of the calculation need not correspond to the geographic pole of Enceladus.

Results: We ran a total of 8 models. Using an ice shell thickness of 70 km, we ran a case each with near-surface heating at the pole and the equator, as well as a corresponding case for each geometry without the near-surface heating. These three cases were repeated with a 40-km thick ice shell. All models have $\eta_0 = 3\times10^{13}$ Pa s, or a Rayleigh number $Ra = 9.2\times10^8$, where

$$\mathrm{Ra} = (\rho g \alpha\, \delta T\, R_s^3) / (\kappa \eta_0) \qquad (2)$$

where ρ is the density, g is the gravity, α is the coefficient of thermal expansion, and δT is the temperature difference across the ice shell at the equator, R_s is the radius of the satellite, and κ is the thermal diffusivity. E = 60 kJ/mol.

In Fig. 1 we show the heating rate and temperature distributions for two cases with a 70-km thick ice shell. The two cases are identical except for 7 GW of near-surface heating in panel (b). Even though the extra south polar heating is confined to the near-surface, the deeper temperature structure is affected. The near-surface heating insulates the interior. The warmer upper mantle in the polar region is weaker and more susceptible to tidal deformation, and the shallow tidal heating is also enhanced in this case.

We also find that the near-surface heating promotes melting. The high temperature in Fig. 1b has resulted in local melting at the base of the ice shell near the south pole at an average rate of 6×10^9 kg/yr, five times the rate as for the case in Fig. 1a.

The surface expression of the near-surface heating is dramatic. The dynamic geoid and topography in the south polar region are much stronger when shear heating is present (Fig. 2a). The variation in topography is mirrored in the elastic thickness, T_e (Fig. 2b) here defined as the depth to the 160 K isotherm.

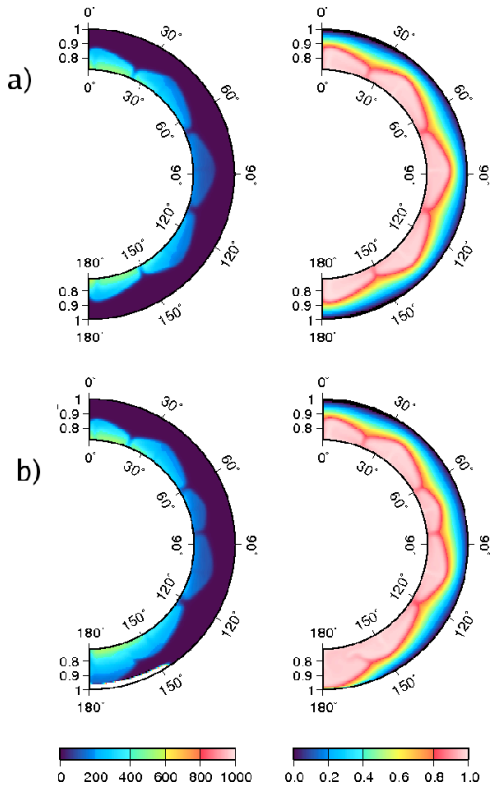

Figure 1: Heating rate in 10^{-9} W m^{-3} (left), and nondimensional temperature (right) for 2D axisymmetric convection cases with tidal dissipation. (a) and (b) are identical except for the inclusion of 7 GW of near-surface heat in the south polar region of (b).

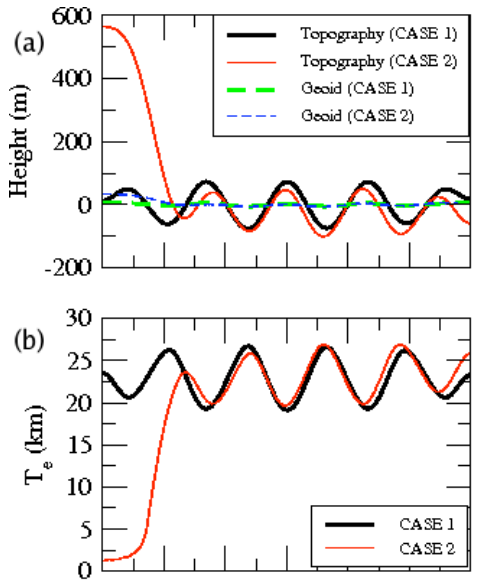

Figure 2: Latitude-dependence of dynamic topography and geoid (a), and elastic thickness T_e (b) for tidally-heated convection models with and without near-surface heating.

Discussion: Planetary reorientation is a possible result of an upwelling diapir such as that shown in Fig. 1b [9]. The mass anomaly due to the buoyant upwelling is compensated by dynamic topography at the surface (Fig. 2a). However, in the presence of a lithosphere, most of this buoyancy is supported elastically, and the dynamic topography is reduced, resulting in a net negative geoid at the south pole.

The negative geoid may be further enhanced by the melting of the ice shell. The volume change associated with the melting of ice I will result in topographic subsidence of the melt region [15], consistent with the observation that the south polar terrain is depressed [1]. The melting rate for the case shown in Fig. 1b results in 6.7×10^4 km of melted ice, for a volume change of 5400 km^3, corresponding to an average of 78 m subsidence in the south polar terrain.

A negative degree-2 geoid will drive poleward reorientation of the geoid anomaly, but this TPW is resisted by the fossil rotational and tidal bulges which are functions of T_e 16]. For the case in Fig. 1b, with T_e = 23 km and 78 m of subsidence, we predict about 9º of TPW. Sustained melting over a greater time span can increase the subsidence and amount of TPW, but ~500 m of subsidence would be required to drive 90º of TPW, an amount that is not observationally supported [1]. This suggests that the south polar region formed near its present location. However, additional physics and chemistry not considered here may have important effects. For example, partial melting may remove impurities from the upwelling, increasing its buoyancy [17] and thus the geoid anomaly without requiring implausible amounts of subsidence topography to drive polar reorientation.

References: [1] Thomas, P. C. et al. (2007) *Icarus* 190, 573-584. [2] Spencer, J. R. et al. (2006) *Science* 311, 1401-1405. [3] Porco, C. C. et al. (2006) *Science* 311, 1393-1401. [4] Roberts, J. H. and F. Nimmo (2008) *Icarus*, in press. [5] Hoppa, G. et al. (1999) *Icarus* 141, 287-298. [6] Nimmo, F. and E. Gaidos (2002) *JGR* 107, 5-1. [7] Nimmo, F. et al. (2007) *Nature* 447, 289-291. [8] Han, L. and A. P. Showman (2007) *LPSC* 38, 2277. [9] Nimmo, F. and R. T. Pappalardo (2006) *Nature* 441, 614-616. [10] Tobie, G. et al. (2005) *Icarus* 177, 534-549. [11] Sabadini, R. and B. Vermeersen (2004) *Global Dynamics of the Earth*, Kluwer Acad. Pub., Dordrecht. [12] Roberts, J. H. and S. Zhong. (2004) *JGR* 109, E03009. [13] Ojakangas, G. W. and D. J. Stevenson (1989) *Icarus* 81, 220-241. [14] Sotin, C. et al. (2002) *GRL* 29, 74-1. [15] Collins, G. C. and J. C. Goodman (2007) *Icarus* 189, 72-82. [16] Matsuyama, I. and F. Nimmo (2008) *Icarus*, in press. [17] Pappalardo, R. T. and A. C. Barr (2004) *GRL* 31, 1701.